Bioresource Technology 399 (2024) 130625

Contents lists available at ScienceDirect

Bioresource Technology

journal homepage: www.elsevier.com/locate/biortech

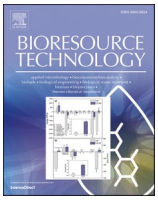

Modelling of anaerobic digestion of microalgae biomass: Effect of overloading perturbation

Silvia Greses [a,*], Julie Jimenez [b], Cristina González-Fernández [a,c,d], Jean-Philippe Steyer [b]

[a] Biotechnological Processes Unit, IMDEA Energy, Avda. Ramón de la Sagra 3, 28935 Móstoles, Madrid, Spain
[b] LBE, Univ Montpellier, INRAE, 102 avenue des Etangs, F-11100 Narbonne, France
[c] Department of Chemical Engineering and Environmental Technology, School of Industrial Engineering, University of Valladolid, Dr. Mergelina, s/n, Valladolid 47011, Spain
[d] Institute of Sustainable Processes, Dr. Mergelina, s/n, Valladolid 47011, Spain

HIGHLIGHTS

- Original ADM1 can only represent anaerobic digestion in the absence of perturbation.
- The co-occurring of acids and ammonium accumulation distort the inhibitions effect.
- Recoverable overload was observed after loading higher than 7 g COD $L^{-1}d^{-1}$.
- New inhibitions by product are required to improve ADM1 predictability.
- Modified ADM1 keep the suitability to fit the data without perturbance.

GRAPHICAL ABSTRACT

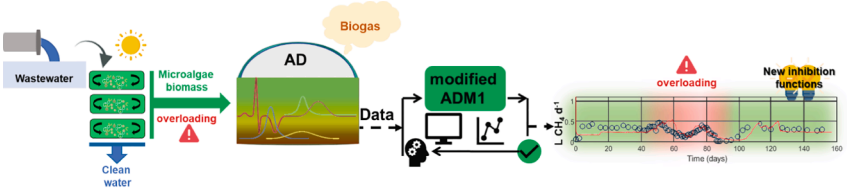

ARTICLE INFO

Keywords:
Process perturbation
Biogas failure
Inhibition by product
ADM1
Volatile fatty acids
Organic loading rate

ABSTRACT

Anaerobic digestion (AD) of microalgae is an intriguing approach for bioenergy production. The scaling-up of AD presents a significant challenge due to the systematic efficiency losses related to process instabilities. To gain a comprehensive understanding of AD behavior, this study assessed a modified version of the anaerobic digestion model No1 (ADM1) + Contois kinetics to represent microalgae AD impacted by overloading. To this end, two new inhibition functions were implemented: inhibition by acetate for acidogenesis/acetogenesis and total volatile fatty acids for hydrolysis. This proposed ADM1 modification (including Contois kinetics) simulated AD behavior during the stable, disturbed and recovery periods, showing that the inhibition functions described in the original ADM1 cannot explain the AD performance under one of the most common perturbations at industrial scale (overloading). The findings underscore the importance of refining the inhibitions present in original ADM1 to better capture and predict the complexities of microalgae AD against overloading.

1. Introduction

The increasing energy demand is drawing attention to the development of renewable sources to mitigate energy insecurity and the rise of global energy prices. In 2022, Europe experienced an energy demand increase averaging 1–2 % (Ritchie et al., 2022), which provoked an energy supply risk along with an alarming rise of 40 % oil prices and over 130 % of gas price (Davenport and Wayth, 2023). In this context,

* Corresponding author.
E-mail address: silvia.greses@imdea.org (S. Greses).

https://doi.org/10.1016/j.biortech.2024.130625
Received 10 January 2024; Received in revised form 19 March 2024; Accepted 19 March 2024
Available online 20 March 2024

anaerobic digestion (AD) has been positioned as a focal point of technological advancement since a significant source of renewable energy (biogas) can be supplied through this biotechnology. AD is a well-known process wherein a complex and synergic microbiome is able to transform a wide range of organic residues into biogas, contributing to a circular economy. Among the residual organic biomass employed as feedstock, microalgae biomass produced during wastewater treatment (WWT) using photobiotechnologies has been extensively studied in the last decade. These studies highlights the numerous advantages of integrating both technologies, microalgae-based WWT and biogas production via AD of microalgae culture in wastewater (Bele et al., 2023). Despite the high methanogenic potential of microalgae biomass (Marques et al., 2019; Olsson et al., 2014; Rusten and Sahu, 2011), long-term biogas production has not been optimized at large-scale since process instability is often encountered (Cavinato et al., 2017; European Commission, 2022, 2018). The scaling-up of AD processes leads to a systematic loss of efficiency, which is normally related to unexpected perturbations. Among the unforeseen events that can occur at industrial scale, those related to the upstream technology (microalgae culture) are the most difficult ones to control and mitigate. In this regard, changes in microalgae composition, population and concentration are commonly found in microalgae-based WWT (Morillas-España et al., 2022). These unavoidable variations are mainly related to seasonal changes in terms of weather conditions and wastewater composition (Morillas-España et al., 2020), which subsequently alter the harvesting/dewatering steps and AD feeding. Besides, clogged pipes, broken or malfunctioning pumps and controllers are also commonly found in industrial facilities, aggravating the AD perturbation. Upon such events, microbial communities are affected and the methane production yield becomes unstable, ending up in biogas production failure when corrective actions are not taken immediately. Anticipating failure is crucial for applying prevention and/or mitigation countermeasures that ensure process stability and technology profitability in the long term. To this end, dynamical mathematical modeling can be used as a tool to understand and predict process behavior. One of the most recognized models to describe the main bioreactions occurring in AD is the Anaerobic Digestion Model No.1 (ADM1) developed by the IWA group (Batstone et al., 2002a,b). Previous investigations have demonstrated that a modified version of ADM1 that includes Contois kinetics better represents the hydrolysis stage in AD of microalgae biomass (Mairet et al., 2011; Passos et al., 2015). However, those investigations only addressed conventional AD of microalgae under optimal conditions and without considering potential perturbances, such as a system overloading. An AD overload normally leads to organic acids accumulation that provokes the inhibition of the process by a pH drop. Although previous authors assessed ADM1 to reproduce the inhibition by organic acids (Mo et al., 2023, Vavilin et al., 2008) the different microbial robustness encountered among hydrolytic, acidogenic, acetogenic and methanogenic microorganism against inhibitors has been neglected. The novelty of this study was to modify ADM1 to describe AD of microalgae including process failure and recovery, considering the simultaneous inhibition of various steps of AD when the process was subjected to an overload. For such a purpose, the modification of ADM1 and its corresponding validation was conducted by using the experimental data retrieved from the microalgae AD subjected to an organic loading rate shock in reactors operated in continuous mode.

2. Material and Methods

2.1. Microalgae biomass used as feedstock

Microalgae biomass (*Scenedesmus* > 90 %) cultured in wastewater was used as a feedstock (supplied by Centro IFAPA, La Cañada-Almería, Spain). *Scenedesmus* possesses a rigid cell-wall that exhibit high resistance to biological degradation (Passos et al., 2014a). In order to avoid problems related to the cell wall disintegration during the microalgae conversion into biogas, an enzymatic pretreatment was applied following the procedure described by Mahdy et al. (2015). Table 1 shows the microalgae biomass characterization in terms of total and soluble chemical oxygen demand (TCOD and SCOD, respectively), total solids (TS), volatile solids (VS), ammonium ($N\text{-}NH_4^+$), total nitrogen (TN), protein, carbohydrate, lipids, ash and biochemical methane potential (BMP).

To apply an OLR shock, the microalgae concentration in the influent was dynamically changed from 29.6 g $TCOD{\cdot}L^{-1}$ (corresponding to an OLR of 1.5 g $TCOD{\cdot}L^{-1}{\cdot}d^{-1}$) to 126.1 g $TCOD{\cdot}L^{-1}$ (corresponding to an OLR of 7 g $TCOD{\cdot}L^{-1}{\cdot}d^{-1}$). Accordingly, a concomitant increase in TN influent took place (from 1.6 to 5.9 g $N{\cdot}L^{-1}$). It is important to clarify that the influent flow rate was not modified throughout the experiment, provoking the OLR increase only by rising the COD concentration in microalgae biomass used as feedstock.

2.2. Experimental setup

To evaluate microalgae AD behavior against OLR perturbance, four continuous stirred tank reactors (CSTRs) were run in parallel. Two CSTRs (biological replicates) were used as control and two CSTRs (biological replicates) were subjected to an OLR perturbation. The 1.5-L-CSTRs (0.5 L of headspace) were inoculated with sludge collected from a conventional anaerobic digester located in a wastewater treatment plant (Arroyo del Soto – Móstoles, Madrid, Spain). A magnetic stirrer (Hei-PLATE Mix 20L, Heidolph, DE) was used to homogenize the fermentation broth in the CSTRs. The temperature was controlled using a thermostatic water bath (F12-ED v2.0, Julabo, DE). Temperature, pH and oxidation–reduction potential were online monitored using sensors installed in each CSTRs (C3040 – Consort, BE). The biogas production was daily measured by connecting the headspace of the CSTRs to a flow meter (MilliGascounters – Ritter, DE). The four CSTRs were initially operated under the optimal conditions described for biogas production of pretreated microalgae: 35 °C, an OLR of 1.5 g $TCOD{\cdot}L^{-1}{\cdot}d^{-1}$ and a hydraulic retention time of 18 days (Mahdy et al., 2015). Once AD reached the steady state, two CSTRs were used as control (replicates) wherein no perturbance was applied, and two CSTR (replicates) were subjected to a stepwise OLR increase from 1.5 to 7 g $TCOD{\cdot}L^{-1}{\cdot}d^{-1}$ for 45 days to simulate an uncontrolled overload. To recover the process, optimal conditions were again implemented in the perturbed CSTRs after 45 days.

2.3. Analytical methods

Microalgae composition was characterized in terms of TCOD, SCOD, TS, VS, ash, NH_4^+-N and total Kjeldahl nitrogen (TKN) according to Standard Methods (APHA, 2017). The phenol–sulfuric method (Dubois et al.,1956) was used to determine the content of carbohydrates, while protein concentration was calculated using a TKN-to-protein conversion factor of 5.95 (González-López et al., 2010).The percentage of lipids (dry

Table 1
Characterization of pretreated microalgae biomass used as feedstock (mean ± standard deviation).

Parameter	Microalgae biomass	
TCOD ($g{\cdot}L^{-1}$)	29.6	±2.0
SCOD (%)	41.2	±5.9
TS (%w/w)	1.71	±0.24
VS (%)*	86.5	±3.0
TN (%)*	10.1	±0.1
$N\text{-}NH_4^+$ ($g\ N{\cdot}L^{-1}$)	0.7	±0.2
Carbohydrate (%)*	17.8	±0.5
Protein (%)*	53.1	±2.4
Lipid (%)*	10.2	±1.0
Ash (%)*	13.5	±3.0
BMP ($mLCH_4{\cdot}g\ COD_{influent}^{-1}$)	196.7	±6.4

* Percentage calculated based on dry matter content.

matter basis) was determined by subtracting the percentage of carbohydrate, protein and ash from 100 %. BMP and the corresponding microalgae biodegradability were obtained according to the procedure described by Raposo et al. (2011).

The CSTRs were monitored by analyzing TCOD, SCOD, TS, VS and NH_4^+-N in the effluent as described above and compared with the influents fed in the digesters. Metabolites including acetic acid (HAc), propionic acid (HPro), isobutyric acid (isoHBu), butyric acid (HBu), isovaleric acid (isoHVal), valeric acid (HVal) and caproic acid (HCa), were determined using a high performance liquid chromatograph (1260 HPLC, Agilent) equipped with a refractive index detector and following the conditions described by Greses et al. (2021). A gas chromatograph (Clarus 580 GC, PerkinElmer) equipped with a thermal conductivity detector was used to analyses the biogas composition (CO_2, CH_4, N_2 and H_2). The detailed conditions of GC were previously described by Greses et al. (2021).

2.4. Modelling approach

ADM1 mathematically represents the disintegration, hydrolysis, acidogenesis, acetogenesis and methanogenesis steps of AD, including the physical–chemical reactions (liquid–gas transfer, acid-base reaction) and the inhibition phenomena (Batstone et al., 2002a,b). As starting point, the ADM1 modification proposed by Mairet et al. (2011) was used to predict microalgae AD behavior against an OLR perturbance. Mairet et al. (2011) described the hydrolysis step involved in microalgae AD using the Contois kinetic (Eq. (1) instead of the first-order kinetics (Eq. (2) implemented in the original ADM1. These equations might be defined as follows using carbohydrates as an example:

$$\rho_{CH} = k_{hyd,CH} \cdot \frac{X_{CH}}{K_{S,CH} \cdot X_{su} + X_{CH}} \cdot X_{su} \quad (1)$$

$$\rho_{CH} = k_{hyd,CH} \cdot X_{CH} \quad (2)$$

where ρ_{CH} represents the hydrolysis rate of carbohydrates, $k_{hyd,CH}$ is the hydrolysis constant for carbohydrates, X_{CH} is the carbohydrate concentration, X_{su} is the hydrolytic microorganisms concentration and $K_{S,CH}$ is the half saturation constant of carbohydrate hydrolysis. The Contois model considers the amount of substrate per biomass (microorganisms) unit. This model is commonly used when hydrolysis is identified as the limiting step of AD due to the substrate complexity (which is the case of microalgae (Passos et al., 2014a)), or when the digestion is conducted under high substrate-to-biomass ratio (organic overloading) (Vavilin et al., 2008). MATALB 2021® was used to simulate ADM1 modifications by means of the implementation of Rosen and Jeppsson (2006).

2.4.1. Model input

To accurately model the experimental data, detailed input values obtained from the feedstock characterization are required. Microalgae biomass composition (Table 1) was used to calculate the model input and the stoichiometric parameters for the CSTRs in the absence of perturbance (Table 2), considering the particulate organic matter distribution (protein, lipids, carbohydrates and ashes) in terms of COD equivalent and its biodegradability (BMP).

The characterization shown in Table 2 was also used to determine the initial values of the state variables, as detailed by Jimenez et al. (2020). The model was simulated under continuous conditions until achieving an equilibrium (so-called steady-state). Thereafter, the values resulting from the steady-state served as initial values for state variables.

Regarding the CSTR subjected to the OLR perturbance, $X_{c,in}$, $S_{su,in}$ and $S_{aa,in}$ were dynamically changed once the process reached the steady state to represent the deliberately imposed organic matter content increase in the influent. In the OLR perturbance, the same initial state variables as Control CSTR were used.

Table 2
Model input characterization.

	Parameter	Description	Value
Input parameters	$S_{su,in}$ (kg sCOD·m^{-3})	Monosaccharides	5.26
	$S_{aa,in}$ (kg sCOD·m^{-3})	Amino acids	5.87
	$S_{IC,in}$ (M)	Inorganic carbon	0.019*
	$S_{IN,in}$ (M)	Inorganic nitrogen	0.011*
	$S_{I,in}$ (kg sCOD·m^{-3})	Soluble inerts	1.08
	$X_{c,in}$ (kg pCOD·m^{-3})	Complex particulate organic matter	17.41
	$S_{cat,in}$ (M)	Cations	0.024*
	$S_{an,in}$ (M)	Anions	0.0065*
Stoichiometric parameters	$f_{sI,xc}$	Soluble inerts from complex organic matter	0
	$f_{xI,xc}$	Particulate inerts from complex organic matter	0.53
	$f_{ch,xc}$	Carbohydrates from complex organic matter	0.088
	$f_{pr,xc}$	Proteins from complex organic matter	0.221
	$f_{li,xc}$	Lipids from complex organic matter	0.161
	N_{xc} (kmol·kg pCOD^{-1})	Nitrogen content of complex organic matter	0.004
	N_I (kmol·kg sCOD^{-1})	Nitrogen content of inerts	0.004

* Mairet et al. (2011).

3. Results and discussion

3.1. Experimental data comparison with process simulation using anaerobic digestion model No.1 modified with Contois model

AD of enzymatically pretreated microalgae biomass was performed for 160 days, evidencing a stable biogas production when perturbances were not applied (control reactors, Fig. 1). As a result, methane yield reached 171.3 ± 12.4 mLCH_4·g $TCOD_{inf}^{-1}$, corresponding to a biodegradability of 48 ± 3 %. These values agreed with previous studies related to microalgae biomass biomethanation via AD using an enzymatic pretreatment (37–52 % biodegradability) (Mahdy et al., 2015), demonstrating the proper functioning of the process in the CSTRs used as control. Conventionally, the degradation of protein-rich feedstock (such as microalgae) leads to a high total ammoniacal nitrogen (TAN) release that might provoke the AD inhibition when the concentration reached a threshold of 1 g TAN·L^{-1} (Capson-Tojo et al., 2020; Anthonisen et al., 1976). This TAN concentration normally results in an AD inhibition by free ammonia nitrogen (FAN) as primary cause since the pH rise and the temperature provoke the equilibrium displacement to the non-ionic form of nitrogen. Although high ammonium concentration was released during microalgae AD (928 ± 71 mg N-NH_4^+·L^{-1}) due to the high protein content in *Scenedesmus* (Table 1), FAN toxicity was not detected. This fact was evidenced by the significant and constant biogas production and the absence of VFAs accumulation, which is a clear indicator of a well-executed AD. The values resulting from the control reactors described a normal microalgae AD behavior since they were in the range of previous studies dealing with microalgae AD. For instance, Mahdy et al. (2015) found a similar methane yield (128.4 ± 15.3 mLCH_4·g $TCOD_{inf}^{-1}$), under analogous conditions and microalgae pretreatment. This methane yield also fall within the range of previous investigation studying biogas production from microalgae subjected to a different disruption pretreatments (126–170 mLCH_4·g $TCOD_{inf}^{-1}$) (Mendez et al., 2015; Passos et al., 2014b). Thus, the conventional microalgae AD performance compared with previous studies suggested that the ADM1 modified with Contois model could satisfactorily simulate the process, as Mairet et al. (2011) proposed. Although these authors also

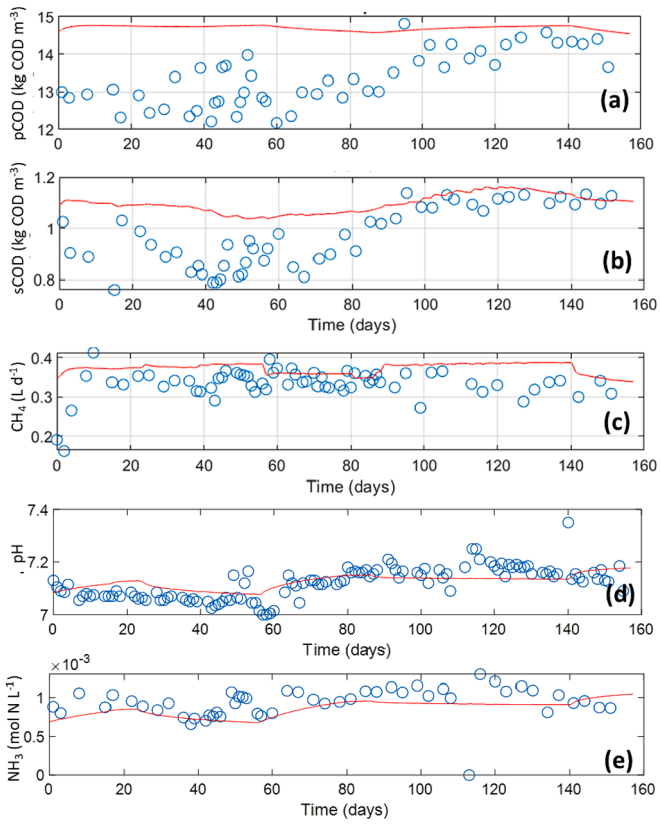

Fig. 1. Time evolution of (a) particulate COD, (b) soluble COD, (c) methane production (d) pH and (e) free ammonia in control CSTRs. Experimental data (o). Predicted data (-) using ADM1 with Contois model.

performed microalgae AD, the parameters were calibrated for raw microalgae. Considering that an enzymatic pretreatment was applied in the present study, a recalibration of the model was required. This pretreatment enhanced the disintegration step, requiring thereby to adjust the disintegration constant value (*kdis*) from 0.5 for raw microalgae (Mairet et al., 2011) to 1.0 for pretreated microalgae. The high *kdis* value allowed to regulate the downstream processes by the hydrolysis step, which also resulted in a different calibration of the hydrolysis constant for carbohydrates ($k_{hyd,ch}$), proteins ($k_{hyd,pr}$) and lipids ($k_{hyd,li}$) (Table 3).

Once the kinetic parameters were calibrated for the pretreated microalgae biomass, the implementation of the Contois model was able to describe the experimental data in the control reactors (Fig. 1). This model predicted not only the daily methane production but also the sCOD and particulate COD (pCOD) present in the CSTR, confirming the suitability of the hydrolysis model using Contois kinetics to represent microalgae AD. To improve the pCOD simulation, it is important to highlight that the inert fraction fed in the CSTRs (Table 2) was modified according to the biodegradability resulting from control reactors when the process reached the steady state. Although BMP is useful to evaluate a residue biodegradability, this batch test normally results in an overestimation when compared to reactors operated in continuous mode since the effect of operational parameters on microorganism growth is not taken into account (Alzate et al., 2012). Hence, the inert fraction obtained once the control CSTRs reached the steady state (0.53) was used instead of the one resulting from BMP test (0.44). This adjustment yielded a more representative simulation compared to the results obtained using BMP assay data (see supplementary material) in terms of COD, methane production, ammonia and pH evolution.

Table 3
Kinetic parameter values from ADM1 with/without modifications.

Kinetic parameter	Description	ADM1[1]	This study
k_{dis} (d^{-1})	Maximum specific disintegration rate	0.5	1
$k_{hyd,ch}$ (d^{-1})	Maximum specific hydrolysis rate of carbohydrates	10	1.18
$K_{s,ch}$ (kg COD·m^{-3})	Half saturation constant of carbohydrate hydrolysis	0.5	0.5
$k_{hyd,pr}$ (d^{-1})	Maximum specific hydrolysis rate of protein	10	0.5
$K_{s,pr}$ (kg COD·m^{-3})	Half saturation constant of protein hydrolysis	0.5	0.26
$k_{hyd,li}$ (d^{-1})	Maximum specific hydrolysis rate of lipid	10	1.07
$K_{s,li}$ (kg COD·m^{-3})	Half saturation constant of protein hydrolysis	0.5	0.49

Note: Parameters not described in Table 3 remained as in the original ADM1.
[1] Hydrolysis using first order kinetics.

However, the good performance of ADM1 with the Contois model in describing microalgae AD could not be extended to the process subjected to an overload. The OLR perturbance provoked a biogas decline after 9 experimental days, reaching the complete AD inhibition after 45 days of shock. The process failure resulted in a VFAs accumulation of 29.2 g COD·L^{-1} (mainly HAc, HPro, HBu and HVal), which is a common feature of inhibited AD systems (Basak et al., 2021). Accordingly, a SCOD accumulation of 39.3 g COD·L^{-1} was also determined, indicating that a fraction of SCOD (10.1 g·L^{-1}) remained unconverted into VFAs. This fact denoted that not only methanogenesis but also previous steps of AD were affected by the perturbance. As Fig. 2 shows, ADM1 predicted a methane rise when the OLR increased, whereby a total biogas inhibition was not reproduced (Fig. 2j). Although particulate organic matter was fairly well simulated by ADM1 (Fig. 2a), SCOD and VFAs were underestimated, predicting only HAc accumulation (Fig. 2f). The absence of other VFAs in the simulation was attributed to the methanogens consumption to produce methane, as no inhibitory factors were present. Accordingly, the model simulated a methanogenic archaea growth without exhibiting a perturbation (see supplementary material), which gave rise to a lower predicted value of VFAs and an overestimation of biogas production.

As an attempt to improve model predictability in the CSTRs subjected to an OLR shock, the maximum uptake rates (k_m) for HPro, HBu and HVal were adjusted. Hence, a notable reduction of k_m allowed to increase the accumulation of those VFAs while limiting their conversion into methane. This adjustment also provoked a decrease in HAc that was corrected by reducing the k_m of HAc as well. Nevertheless, the model did not predict the accumulated sCOD that was not transformed into VFAs. This fact resulted from the initial sCOD transformation into HAc to ultimately produce methane, leading to an overestimation of biogas production too (see supplementary material). These results evidenced that ADM1 with Contois model was not able to represent the process dynamics in presence of perturbances. As a matter of fact, a persistent VFAs accumulation of 2 g COD·L^{-1} was predicted by the model when control reactors were simulated again with the modified k_m values, confirming that k_m variations were not the key strategy to increase model accuracy.

To simulate a biogas decline and a VFAs accumulation, the AD process has to experience an inhibition. According to ADM1, biogas production can be inhibited by nitrogen limitation (<0.0001 M of N), NH_3 (>0.0018 M), pH or high H_2 partial pressure ($3.5{\cdot}10^{-6}$ – $1{\cdot}10^{-5}$), while acidogenesis and acetogenesis can be also inhibited by pH and H_2 (Batstone et al., 2002a,b). Although a slight inhibition by NH_3 was predicted (I_{NH3} = 0.75–0.5) during the organic overloading, pH oscillations were not outside the conventional boundaries (6–7). As previously explained, AD of microalgae releases a high amount of ammonium as a consequence of protein degradation. Ammonium provokes a pH rise that normally results in a NH_3 increase, exhibiting a direct negative response in biogas production (Capson-Tojo et al., 2020). However, in this study, the high VFAs accumulation contributed to an increase in H^+ ions, preventing the pH rise due to the high accumulation of ammoniacal nitrogen. Thus, the co-occurrence of both factors prevented the

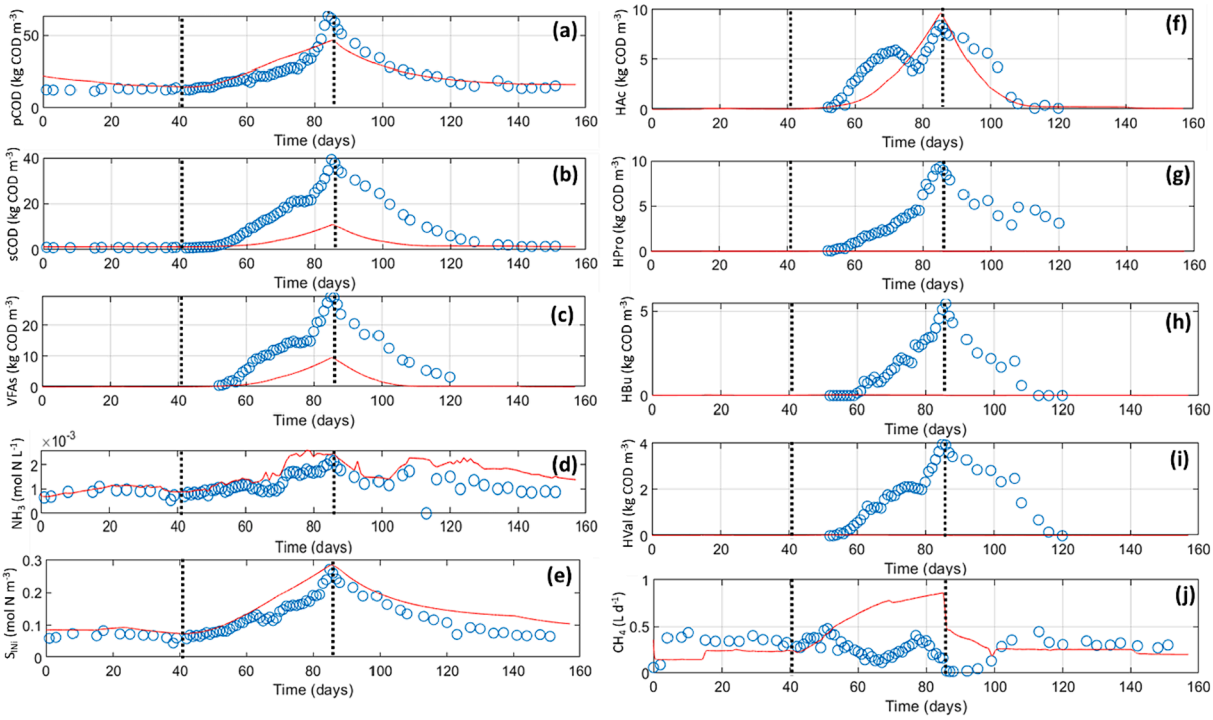

Fig. 2. Time evolution of (a) particulate COD, (b) soluble COD, (c) volatile fatty acids (d) free ammonia, (e) soluble inorganic nitrogen (mainly ammonium), (f) acetate, (g) propionate, (h) butyrate, (i), valerate and (j) methane production in the CSTRs subjected to an OLR perturbance. Experimental data (o). Predicted data (-) using ADM1 with the Contois model. The dotted lines represent the starting and ending days of the OLR perturbance.

inhibition by free ammonia. Likewise, the significant buffer capacity provided by the high ammonium content in the process also prevented a critical pH drop caused by high VFAs accumulation. Considering that there was no nitrogen limitation due to the presence of high ammonium, and H_2 was not detected in the CSTRs subjected to an OLR shock, the inhibition factors described in ADM1 cannot explain the AD behavior against an OLR shock. These evidences agreed with the model prediction in which, H_2 production take place in percentages lower than the limit of detection of the GC and no significant inhibition by H_2 was simulated. As a matter of fact, the microbiome simulation resulted from ADM1 using Contois model did not evidence the inhibition of any group of bacteria as the OLR increased (only a slight inhibition of acetate consumers by FAN), confirming that the current inhibition factors were not able to reproduce the experimental data retrieved from the AD of microalgae biomass subjected to an overloading. Hence, these results suggested that alternative inhibition factors were required to fit ADM1 to the obtained experimental data.

3.2. Anaerobic digestion model No.1 modification

Since pH has been identified as one of the most inhibitory factors for methanogenic population (Eryildiz et al., 2020), pH boundaries were the first modification implemented. Biogas production during the OLR shock was in agreement with the pH oscillations, which was confirmed by the principal component analysis (PCA) that revealed a correlation between both data output (pH and methane) retrieved during the perturbation (see supplementary material). This fact might indicate that methanogenesis had a high correlation with this parameter. Although pH was out of inhibition threshold values (6–7) for conventional AD, previous studies demonstrated that AD subjected to extreme conditions (high VFAs and ammonium accumulation) are prone to instability against minor changes (Pasalari et al., 2021). This can support the fact that narrow pH ranges could be detrimental for AD performance. Hence, upper (UL) and lower (LL) limits values were adjusted as Table 4 shows.

Once the pH limits were adjusted, the model allowed to reproduce the methane production shape but the volume was still slightly higher than that obtained experimentally (see supplementary material). Additionally, a simulation mismatch was found in the metabolites concentration since the whole SCOD was transformed into HAc and reaching a maximum concentration of 22 g COD·L^{-1}. This fact evidenced that methanogenesis inhibition was not enough to also simulate the SCOD and VFAs accumulated during the AD overloading. Aiming at enhancing the model fit to the experimental data, new inhibition functions should be included to prevent the metabolization of VFAs into HAc, and also the total SCOD degradation into VFAs.

Table 4
pH limits described in ADM1 with/without modifications.

Parameter	Description	ADM1	This study
$pH_{LL,ac}$	Lower limit of pH inhibition	6	6.8
$pH_{UL,ac}$	Upper limit of pH inhibition	7	7.2

AD inhibition has been traditionally focused on methanogenesis and acetogenesis stages, while hydrolysis and acidogenesis inhibition is normally neglected due to the higher robustness of these microorganisms against process instabilities (Pasalari et al., 2021; Vavilin et al., 2008). Nevertheless, it has been proven that VFAs can also exhibit an inhibitory effect on initial steps of AD. High HAc accumulation can hamper the degradation of longer carbon chain VFAs (HPro, HBu, HVal) into methane precursors (Ramos-Suarez et al., 2021), as well as the hydrolysis of the organic matter (Duong et al., 2022). In this regard, the PCA showed that VFAs (specially HAc) exhibited high correlation with those experimental data retrieved during the total methane production failure, being these parameters (VFAs and HAc) with similar impact to NH_3 in the principal component 1 (see supplementary material).

Some ADM1 modifications have been implemented to simulate the hydrolysis inhibition using an inhibition by total VFA concentration (Normak et al., 2015; Vavilin et al., 2008), or the inhibition of propionate and butyrate uptake considering the HAc concentration in the function (Mo et al., 2023). Those studies modeled the inhibition

separately (hydrolysis or acetogenesis), neglecting the negative simultaneous effect of VFAs in other AD steps. Gavala et al. (2003) proposed the inhibition of hydrolytic, acidogenic and acetogenic bacteria by total VFAs, using a single inhibition function for all the bacterial groups. Nevertheless, the microbiome robustness should be taken into account to predict the AD performance against inhibitions. For instance, the optimal pH for hydrolytic microorganisms has been identified in a range of 4.5–5.5 (Feng et al., 2018), while acidogenic ones thrive optimally at 5.5–6.5 (Bühlmann et al., 2022). This fact suggests that hydrolytic microorganisms tolerate higher VFAs concentrations (corresponding to lower pH values) than acidogens, justifying the high influence of VFAs and HAc on the AD failure determined in the PCA. Hence, to reflect the inhibitory effect of VFAs on different stages of AD, two new inhibition functions were proposed in the present study. Firstly, to model the accumulation of intermediate metabolites (HPro, HBu and HVal), the acidogenesis and acetogenesis were limited introducing an inhibition by product using the non-competitive function described in Equation (3).

$$I_{ac} = \frac{1}{1 + \frac{S_{ac}}{K_{I_{ac}}}} \quad (3)$$

where S_{ac} represents the concentration of HAc as g COD·L^{-1} and K_{Iac} was the inhibition constant that was adjusted to 0.25 g COD·L^{-1}. I_{ac} was included as part of the inhibition factor I_1, I_2, and I_3 described in ADM1 (Table 5). More specifically, I_1 is used in ADM1 to limit the sugars transformation into HAc, HPro and HBu, and amino acids metabolization into HAc, HPro, HBu and HVal, when there is an inhibition by pH or nitrogen limitation. I_2 includes I_1 and an inhibition by H_2 partial pressure, being used to limit the fatty acids, HVal, HBu and HPro uptake. I_3 adds the inhibition by free ammonia to I_1 limiting the HAc transformation into methane. Hence, the application of I_{ac} increases the inhibitory effect on AD as HAc concentration increases.

To model the hydrolysis inhibition by products, a second non-competitive inhibition function (equation (4) was added to the Contois function for carbohydrate, proteins and lipids degradation, which is described as follows:

$$I_{VFAs} = \frac{1}{1 + \frac{S_{ac}+S_{pro}+S_{bu}+S_{val}}{K_{I_{VFAs}}}} \quad (4)$$

where S_{pro}, S_{bu} and S_{val} represented the concentration of HPro, HBu and HVal, respectively (g COD·L^{-1}). The inhibition constant K_{IVFAs} was adjusted to 5 g COD·L^{-1}, which enables hydrolysis inhibition at a higher total VFA concentration than the one required to inhibit the acidogenic and acetogenic steps.

Table 5
Inhibition function in ADM1 with/without modifications.

Inhibition factors	Description	ADM1	This study
I_{pH}	Inhibition by pH	$\exp\left(-3\cdot\left(\frac{pH - pH_{UL}}{pH_{UL} - pH_{LL}}\right)^2\right)_{pH< pH_{UL}}$ 1 $pH>pH_{UL}$	ADM1
$I_{IN,lim}$	Inhibition by nitrogen limitation	$\frac{1}{1 + \frac{K_{S,IN}}{S_{IN}}}$	ADM1
I_{H2}	Inhibition by H_2 partial pressure	$\frac{1}{1 + \frac{S_{H2}}{K_{I,H2}}}$	ADM1
$I_{NH3,Xac}$	Inhibition by free ammonia	$\frac{1}{1 + \frac{S_{NH3}}{K_{I,NH3}}}$	ADM1
I_1	Inhibition of sugars and amino acids uptake	$I_{pH} \cdot I_{IN,lim}$	$I_{pH} \cdot I_{IN,lim} \cdot I_{ac}$
I_2	Inhibition of VFAs uptake	$I_1 \cdot I_{H2}$	*$I_1 \cdot I_{H2}$
I_3	Inhibition of HAc uptake	$I_1 \cdot I_{NH3,Xac}$	*$I_1 \cdot I_{NH3,Xac}$

* These inhibition factors considered the I_{ac} implemented in the I_1 corresponding to this study.

Fig. 3 shows that the implementation of the inhibition functions allowed predicting both the methane production trend (Fig. 3 j) and the performance of soluble metabolites (Fig. 3). A more accurate pCOD was predicted (Fig. 3a) due to the slow hydrolysis imposed in the model when high VFAs concentration are present (such is the case of the organic overloading perturbances tested herein). Given VFAs are in the dissociated form (pKa 4.76–4.84) when pH values are close to neutrality, the diffusion through cell membrane is mainly limited to secondary cell transporters, such as H^+-monocarboxylate (Warnecke and Gill, 2005). Thus, VFAs compete for the same carrier system than other important monocarboxylates including pyruvate (Poole and Halestrap, 1993), which is essential for cell metabolisms. As VFAs bind the same active sites than pyruvate, the high VFAs accumulation likely competed with pyruvate transport hampering the cells performance. The results obtained from the model suggested that the hydrolysis inhibition function could successfully simulate the negative effect of high VFAs content on particulate organic matter degradation. Moreover, the non-immediate AD recovery was also very well represented since the pCOD accumulation was still present after the shock, being reduced as VFAs were consumed.

Likewise, the model simulated the accumulation of all VFAs and SCOD. As consequence of the implemented product inhibition function in the acidogenesis and acetogenesis steps, the rapid HAc increase attained during the initial days of the shock led to the accumulation of intermediate metabolites. This behavior can be clearly observed in the metabolites evolution between 100 and 120 days (Fig. 3 f-i). As HAc concentration decreased, the reduction of the inhibition enabled acetogens to uptake other VFAs. Concomitantly, the biogas production was also prevented during the OLR perturbance since the high HAc concentration hindered acetoclastic methanogenesis. The model was also able to simulate the bacteria behavior when HAc increase, illustrating that microorganisms involved in HAc degradation to produce methane were the first ones affected by the OLR perturbation, followed by the HPro consumers and HBu/HVal degraders (supplementary material). The inhibition by product of these microorganisms followed a similar explanation given above for hydrolytic bacteria, being the main differences attributed to microbial robustness attending to the intracellular pH and metabolisms. These results allowed to identify an OLR higher than 4 gCOD·L^{-1}·d^{-1} and HAc concentration of 2.6 g·L^{-1} as thresholds for AD inhibition.

The implementation of separate inhibition functions was beneficial in predicting process performance, confirming that hydrolysis inhibition requires a remarkable higher VFAs concentration than acidogenesis/acetogenesis to exhibit a metabolic decline.

The modified model was validated with the experimental results retrieved from control reactors, showing also the ability to simulate microalgae AD in the absence of perturbances. Moreover, a prediction efficiency comparison between original ADM1 and the proposed modification was performed (Fig. 4). The adjustment of the results showed a significant increase in R^2 when using the proposed modification of ADM1. Regarding the methane production, although R^2 also improved when compared to original ADM1, some outliers jeopardized the expected R^2 values. However, root mean square error (RMSE) confirmed the significant enhancement of the prediction efficiency (RMSE 0.2753 in original ADM1 and RMSE 0.0693 in modified ADM1), validating the performance of the proposed ADM1 model modification. It is important to highlight that, giving the high pH buffer capacity in AD of protein-rich feedstocks, these results evidenced the relevance of monitoring HAc to early detect the biogas production failure in this process.

These results demonstrated that the proposed ADM1 modification with new inhibition functions can very satisfactorily represent the collapse resulting from a microalgae AD subjected to an organic overloading, as well as the AD recovery after the shock and the stable AD performance in the absence of perturbations. Moreover, the ADM1

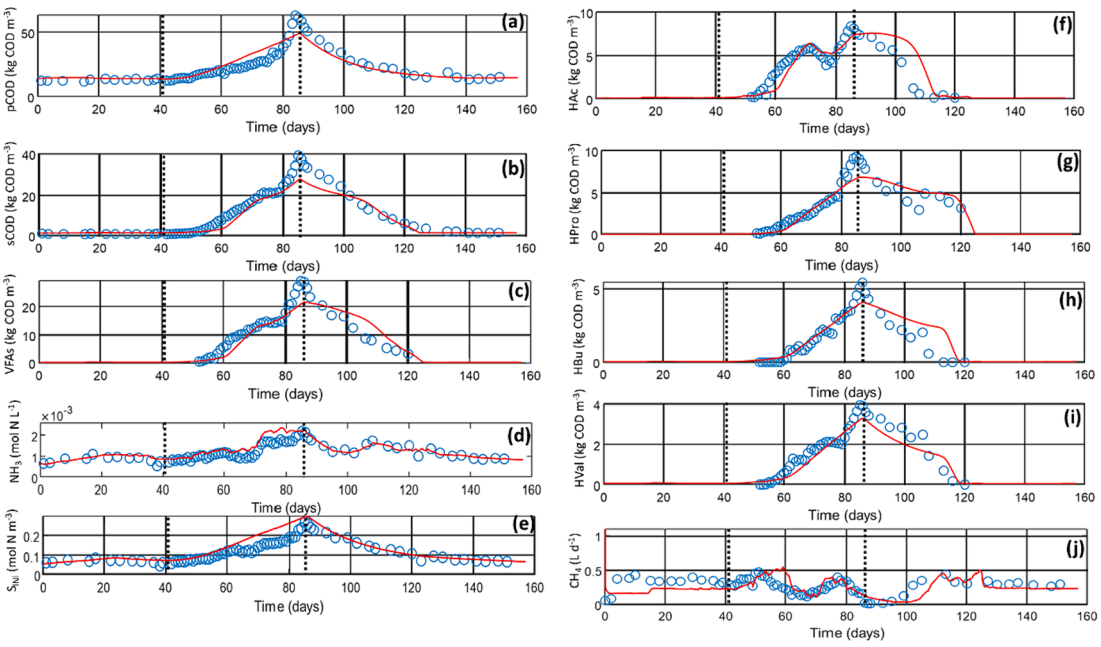

Fig. 3. Time evolution of (a) particulate COD, (b) soluble COD, (c) volatile fatty acids (d) free ammonia, (e) soluble inorganic nitrogen (mainly ammonium), (f) acetate, (g) propionate, (h) butyrate, (i), valerate and (j) methane production in the CSTRs subjected to an OLR perturbance. Experimental data (o). Predicted data (-) using modified ADM1 with new inhibition functions. The dotted lines represent the starting and ending days of the OLR perturbance.

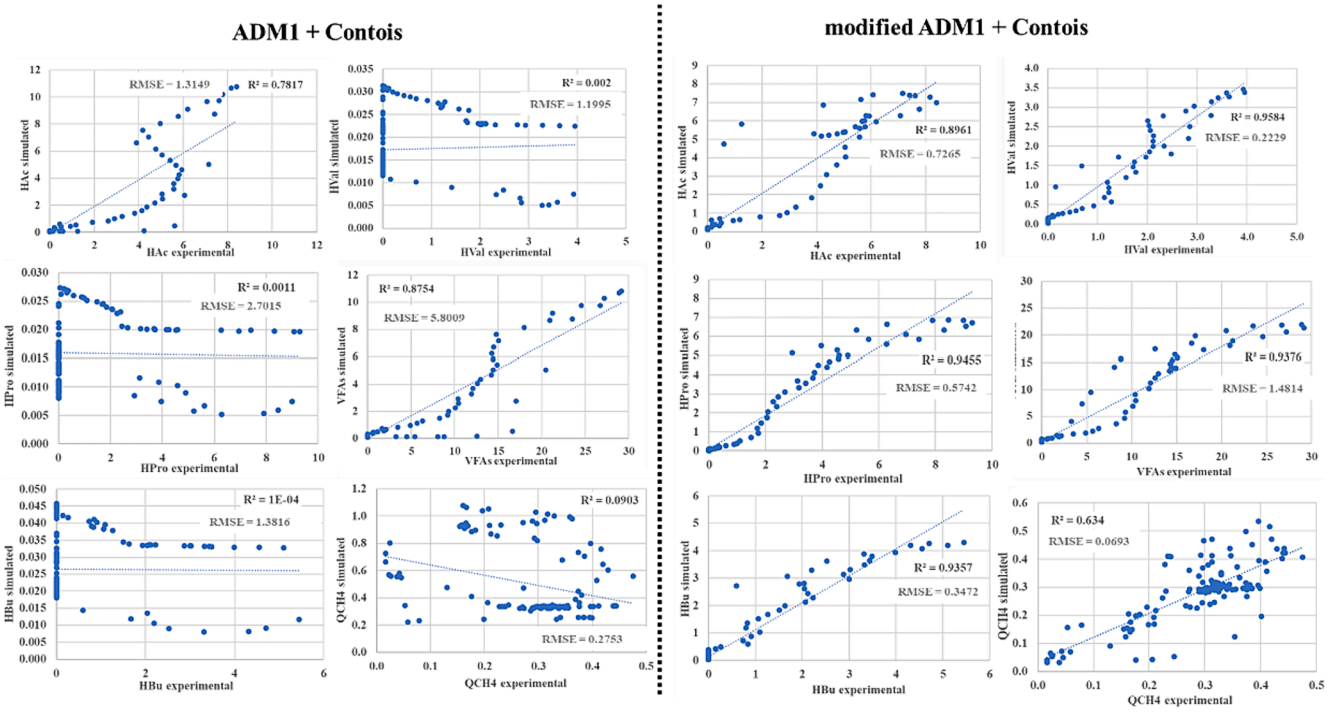

Fig. 4. Comparison of the prediction efficiency using the original ADM1 + Contois model and the proposed modification of ADM1 + Contois model to simulate the CSTR subjected to OLR perturbation in terms of HAc ($gCOD{\cdot}L^{-1}$), HPro ($gCOD{\cdot}L^{-1}$), HBu ($gCOD{\cdot}L^{-1}$), HVal ($gCOD{\cdot}L^{-1}$), VFAs ($gCOD{\cdot}L^{-1}$) and methane production (QCH_4, $mLCH_4{\cdot}d^{-1}$). Experimental data (o). Predicted data (-).

ability to represent not only biogas production failure but also intermediate metabolites accumulation was also demonstrated, which gains relevance in the framework of the biorefineries based on AD as core technology. Since VFAs have been considered valuable building blocks for the industry (Dahiya et al., 2015), predicting their production via AD could help to estimate process yields and confirm the replicability.

4. Conclusions

This study proposed ADM1 modifications to improve microalgae AD prediction, considering not only the conventional behavior but also an organic overloading perturbance. Two new inhibition functions were added to represent the inhibition by product of the hydrolysis, acidogenesis and acetogenesis. This model described very well the data

retrieved from control reactors (no perturbance) and organic overloading (including process recovery), evidencing that the modification did not alter the ADM1 suitability for reproducing a normal microalgae AD performance. This study demonstrated that ADM1 can be improved to increase model predictability against one of the most frequent perturbations found at industrial scale.

CRediT authorship contribution statement

Silvia Greses: Writing – original draft, Methodology, Investigation, Funding acquisition, Formal analysis, Data curation, Conceptualization. **Julie Jimenez:** Writing – review & editing, Validation, Supervision, Resources, Methodology, Formal analysis. **Cristina González-Fernández:** Writing – review & editing, Validation, Supervision, Resources, Investigation, Funding acquisition, Formal analysis, Conceptualization. **Jean-Philippe Steyer:** Writing – review & editing, Validation, Supervision, Resources, Methodology, Formal analysis.

Declaration of competing interest

The authors declare that they have no known competing financial interests or personal relationships that could have appeared to influence the work reported in this paper.

Data availability

Data will be made available on request.

Acknowledgements

This work has been supported by the European Union's Horizon 2020 Research and Innovation Programme through the project PRODIGIO (N. 101007006) and the Unit of Excellence "María de Maeztu" grant with reference number CEX2019-000931-M (2020-2023).

Appendix A. Supplementary data

Supplementary data to this article can be found online at https://doi.org/10.1016/j.biortech.2024.130625.

References

Alzate, M.E., Muñoz, R., Rogalla, F., Fdz-Polanco, F., Pérez-Elvira, S.I., 2012. Biochemical methane potential of microalgae: Influence of substrate to inoculum ratio, biomass concentration and pretreatment, Bioresource Technology. Elsevier Ltd. https://doi.org/10.1016/j.biortech.2012.06.113.

Anthonisen, A.C., Loehr, R.C., Prakasam, T.B.S., Srinath, E.G., 1976. Inhibition of nitrification and nitrous acid compounds. J. Water Pollut. Control Fed. 48, 835–852 https://doi.org/https://www.jstor.org/stable/25038971.

APHA, AWWA, WEF, 2017. Standard Methods for the Examination of Water and Wastewater, 23rd ed., American Public Health Association, Washingto, DC, USA. https://doi.org/ISBN 9780875532356.

Basak, B., Patil, S.M., Saha, S., Kurade, M.B., Ha, G.S., Govindwar, S.P., Lee, S.S., Chang, S.W., Chung, W.J., Jeon, B.H., 2021. Rapid recovery of methane yield in organic overloaded-failed anaerobic digesters through bioaugmentation with acclimatized microbial consortium. Sci. Total Environ. 764, 144219 https://doi.org/10.1016/j.scitotenv.2020.144219.

Batstone, D., Keller, J., Angelidaki, I., Kalyuzhnyi, S.G.P., Pavlostathis, A., Sanders, W., Siegrist, H., Vavilin, V., 2002a. Industrial applications of the IWA anaerobic digestion model No. 1 (ADM1). Water Sci. Technol. 47, 199–206. https://doi.org/10.2166/wst.2003.0647.

Batstone, D.J., Keller, J., Angelidaki, I., Kalyuzhnyi, S.V., Pavlostathis, S.G., Rozzi, A., Sanders, W.T., Siegrist, H., Vavilin, V.A., 2002b. Anaerobic Digestion Model No. 1. Water Sci. Technol. 45, 65–73.

Bele, V., Rajagopal, R., Goyette, B., 2023. Closed loop bioeconomy opportunities through the integration of microalgae cultivation with anaerobic digestion: A critical review. Bioresour. Technol. Reports 21, 101336. https://doi.org/10.1016/j.biteb.2023.101336.

Bühlmann, C.H., Mickan, B.S., Tait, S., Batstone, D.J., Mercer, G.D., Bahri, P.A., 2022. Lactic acid from mixed food waste fermentation using an adapted inoculum: Influence of pH and temperature regulation on yield and product spectrum. J. Clean. Prod. 373, 133716 https://doi.org/10.1016/j.jclepro.2022.133716.

Capson-Tojo, G., Moscoviz, R., Astals, S., Robles, Steyer, J.P., 2020. Unraveling the literature chaos around free ammonia inhibition in anaerobic digestion. Renew. Sustain. Energy Rev. 117, 109487 https://doi.org/10.1016/j.rser.2019.109487.

Cavinato, C., Ugurlu, A., de Godos, I., Kendir, E., Gonzalez-Fernandez, C., 2017. Biogas production from microalgae. In: Microalgae-Based Biofuels and Bioproducts: from Feedstock Cultivation to End-Products, pp. 155–182. https://doi.org/10.1016/B978-0-08-101023-5.00007-8.

European Commission, 2018. A sustainable Bioeconomy for Europe: strengthening the connection between economy, society and the environment. Publications Office. https://doi.org/https://data.europa.eu/doi/10.2777/792130.

European Commission, 2022. The Bioeconomy - Glimpses of the future from the BOHEMIA study. https://doi.org/10.4324/9781003103011.

Dahiya, S., Sarkar, O., Swamy, Y.V., Venkata Mohan, S., 2015. Acidogenic fermentation of food waste for volatile fatty acid production with co-generation of biohydrogen. Bioresour. Technol. 182, 103–113. https://doi.org/10.1016/j.biortech.2015.01.007.

Davenport, J., Wayth, N., 2023. Statistical Review of World Energy 2023, 72nd ed,. Energy Institute.

Dubois, M., Gilles, K.A., Hamilton, J.K., Rebers, P.A., Smith, F., 1956. Colorimetric method for determination of sugars and related substances. Anal. Chem. 28, 350–356. https://doi.org/10.1021/ac60111a017.

Duong, T.H., van Eekert, M., Grolle, K., Tran, T.V.N., Zeeman, G., Temmink, H., 2022. Effect of carbohydrates on protein hydrolysis in anaerobic digestion. Water Sci. Technol. 86, 66–79. https://doi.org/10.2166/wst.2022.200.

Eryildiz, B., Lukitawesa, Taherzadeh, M.J., 2020. Effect of pH, substrate loading, oxygen, and methanogens inhibitors on volatile fatty acid (VFA) production from citrus waste by anaerobic digestion. Bioresour. Technol. 302, 122800 https://doi.org/10.1016/j.biortech.2020.122800.

Feng, K., Li, H., Zheng, C., 2018. Shifting product spectrum by pH adjustment during long-term continuous anaerobic fermentation of food waste. Bioresour. Technol. 270, 180–188. https://doi.org/10.1016/j.biortech.2018.09.035.

Gavala, H.N., Angelidaki, I., Ahring, B.K., 2003. Kinetics and modeling of anaerobic digestion process. Adv. Biochem. Eng. Biotechnol. 81, 57–93. https://doi.org/10.1007/3-540-45839-5_3.

González-López, C.V., del Carmen Cerón García, M., Acién Fernández, F.G., Segovia Bustos, C., Chisti, Y., Fernández, Sevilla, J.M., 2010. Protein measurements of microalgal and cyanobacterial biomass. Bioresour. Technol. 101, 7587–7591. https://doi.org/10.1016/j.biortech.2010.04.077.

Greses, S., Tomás-Pejó, E., González-Fernández, C., 2021. Short-chain fatty acids and hydrogen production in one single anaerobic fermentation stage using carbohydrate-rich food waste. J. Clean. Prod. 284, 124727 https://doi.org/10.1016/j.jclepro.2020.124727.

Jimenez, J., Charnier, C., Kouas, M., Latrille, E., Torrijos, M., Harmand, J., Patureau, D., Spérandio, M., Morgenroth, E., Béline, F., Ekama, G., Vanrolleghem, P.A., Robles, A., Seco, A., Batstone, D.J., Steyer, J.P., 2020. Modelling hydrolysis: Simultaneous versus sequential biodegradation of the hydrolysable fractions. Waste Manag. 101, 150–160. https://doi.org/10.1016/j.wasman.2019.10.004.

Mahdy, A., Mendez, L., Ballesteros, M., González-Fernández, C., 2015. Protease pretreated Chlorella vulgaris biomass bioconversion to methane via semi-continuous anaerobic digestion. Fuel 158, 35–41. https://doi.org/10.1016/j.fuel.2015.04.052.

Mairet, F., Bernard, O., Ras, M., Lardon, L., Steyer, J.P., 2011. Modeling anaerobic digestion of microalgae using ADM1. Bioresour. Technol. 102, 6823–6829. https://doi.org/10.1016/j.biortech.2011.04.015.

Marques, A.L., Araújo, O.Q.F., Cammarota, M.C., 2019. Biogas from microalgae: an overview emphasizing pretreatment methods and their energy return on investment (EROI). Biotechnol. Lett. 41, 193–201. https://doi.org/10.1007/s10529-018-2629-x.

Mendez, L., Mahdy, A., Ballesteros, M., González-Fernández, C., 2015. Biomethane production using fresh and thermally pretreated Chlorella vulgaris biomass: A comparison of batch and semi-continuous feeding mode. Ecol. Eng. 84, 273–277. https://doi.org/10.1016/j.ecoleng.2015.09.056.

Mo, R., Guo, W., Batstone, D., Makinia, J., Li, Y., 2023. Modifications to the anaerobic digestion model no. 1 (ADM1) for enhanced understanding and application of the anaerobic treatment processes – A comprehensive review. Water Res. 244, 120504. https://doi.org/10.1016/j.watres.2023.120504.

Morillas-España, A., Lafarga, T., Gómez-Serrano, C., Acién-Fernández, F.G., González-López, C.V., 2020. Year-long production of Scenedesmus almeriensis in pilot-scale raceway and thin-layer cascade photobioreactors. Algal Res. 51, 102069 https://doi.org/10.1016/j.algal.2020.102069.

Morillas-España, A., Lafarga, T., Sánchez-Zurano, A., Acién-Fernández, F.G., González-López, C., 2022. Microalgae based wastewater treatment coupled to the production of high value agricultural products: Current needs and challenges. Chemosphere 291. https://doi.org/10.1016/j.chemosphere.2021.132968.

Normak, A., Suurpere, J., Suitso, I., Jõgi, E., Kokin, E., Pitk, P., 2015. Improving ADM1 model to simulate anaerobic digestion start-up withinhibition phase based on cattle slurry. Biomass and Bioenergy 80, 260–266. https://doi.org/10.1016/j.biombioe.2015.05.021.

Olsson, J., Feng, X.M., Ascue, J., Gentili, F.G., Shabiimam, M.A., Nehrenheim, E., Thorin, E., 2014. Co-digestion of cultivated microalgae and sewage sludge from municipal waste water treatment. Bioresour. Technol. 171, 203–210. https://doi.org/10.1016/j.biortech.2014.08.069.

Pasalari, H., Gholami, M., Rezaee, A., Esrafili, A., Farzadkia, M., 2021. Perspectives on microbial community in anaerobic digestion with emphasis on environmental parameters: A systematic review. Chemosphere 270, 128618. https://doi.org/10.1016/j.chemosphere.2020.128618.

Passos, F., Uggetti, E., Carrère, H., Ferrer, I., 2014a. Pretreatment of microalgae to improve biogas production: A review. Bioresour. Technol. 172, 403–412. https://doi.org/10.1016/j.biortech.2014.08.114.

Passos, F., Hernández-Mariné, M., García, J., Ferrer, I., 2014b. Long-term anaerobic digestion of microalgae grown in HRAP for wastewater treatment. Effect of Microwave Pretreatment. Water Res. 49, 1–9. https://doi.org/10.1016/j.watres.2013.10.013.

Passos, F., Gutiérrez, R., Brockmann, D., Steyer, J.P., García, J., Ferrer, I., 2015. Microalgae production in wastewater treatment systems, anaerobic digestion and modelling using ADM1. Algal Res. 10, 55–63. https://doi.org/10.1016/j.algal.2015.04.008.

Poole, R.C., Halestrap, A.P., 1993. Transport of lactate and other monocarboxylates across mammalian plasma membranes. Am. J. Physiol. - Cell Physiol. 264, 761–782. https://doi.org/10.1152/ajpcell.1993.264.4.c761.

Ramos-Suarez, M., Zhang, Y., Outram, V., 2021. Current perspectives on acidogenic fermentation to produce volatile fatty acids from waste. Rev. Environ. Sci. Biotechnol. 20, 439–478. https://doi.org/10.1007/s11157-021-09566-0.

Raposo, F., Fernández-Cegrí, V., de la Rubia, M.A., Borja, R., Béline, F., Cavinato, C., Demirer, G., Fernández, B., Fernández-Polanco, M., Frigon, J.C., Ganesh, R., Kaparaju, P., Koubova, J., Méndez, R., Menin, G., Peene, A., Scherer, P., Torrijos, M., Uellendahl, H., Wierinck, I., de Wilde, V., 2011. Biochemical methane potential (BMP) of solid organic substrates: Evaluation of anaerobic biodegradability using data from an international interlaboratory study. J. Chem. Technol. Biotechnol. 86, 1088–1098. https://doi.org/10.1002/jctb.2622.

Ritchie, H., Roser, M., Rosado, P., 2022. Energy. Our World Data.

Rosen, C., Jeppsson, U., 2006. Aspects on ADM1 Implementation within the BSM2 Framework. Tech. Rep. 1–37.

Rusten, B., Sahu, A.K., 2011. Microalgae growth for nutrient recovery from sludge liquor and production of renewable bioenergy. Water Sci. Technol. 64, 1195–1201. https://doi.org/10.2166/wst.2011.722.

Vavilin, V.A., Fernandez, B., Palatsi, J., Flotats, X., 2008. Hydrolysis kinetics in anaerobic degradation of particulate organic material: An overview. Waste Manag. 28, 939–951. https://doi.org/10.1016/j.wasman.2007.03.028.

Warnecke, T., Gill, R.T., 2005. Organic acid toxicity, tolerance, and production in Escherichia coli biorefining applications. Microb. Cell Fact. 4, 1–8. https://doi.org/10.1186/1475-2859-4-25.